



**HAL**  
open science

## Fetuin is the key for nanon self-propagation

Eric Chabriere, Daniel Gonzalez, Said Azza, Pierrick Durand, Farooq A. Shiekh, Valérie Moal, Jean-Pierre Baudoin, Isabelle Pagnier, Didier Raoult

### ► To cite this version:

Eric Chabriere, Daniel Gonzalez, Said Azza, Pierrick Durand, Farooq A. Shiekh, et al.. Fetuin is the key for nanon self-propagation. *Microbial Pathogenesis*, 2014, 73, pp.25-30. 10.1016/j.micpath.2014.05.003 . hal-01521187

HAL Id: hal-01521187

<https://hal.univ-lorraine.fr/hal-01521187v1>

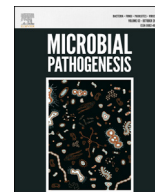
Submitted on 25 Jun 2018

**HAL** is a multi-disciplinary open access archive for the deposit and dissemination of scientific research documents, whether they are published or not. The documents may come from teaching and research institutions in France or abroad, or from public or private research centers.

L'archive ouverte pluridisciplinaire **HAL**, est destinée au dépôt et à la diffusion de documents scientifiques de niveau recherche, publiés ou non, émanant des établissements d'enseignement et de recherche français ou étrangers, des laboratoires publics ou privés.



Distributed under a Creative Commons Attribution - NonCommercial - NoDerivatives 4.0 International License



## Fetuin is the key for nanon self-propagation



Eric Chabrière<sup>a,1</sup>, Daniel Gonzalez<sup>a,1</sup>, Said Azza<sup>a</sup>, Pierrick Durand<sup>b</sup>, Farooq A. Shiekh<sup>a</sup>, Valerie Moal<sup>c</sup>, Jean-Pierre Baudoin<sup>a</sup>, Isabelle Pagnier<sup>a</sup>, Didier Raoult<sup>a,\*</sup>

<sup>a</sup> Aix-Marseille Université, URMITE, UMR CNRS 7278, IRD 198, INSERM U1095, IHU Méditerranée Infection, Faculté de Médecine, 27 Bd Jean Moulin, 13005 Marseille, France

<sup>b</sup> Université de Lorraine, CRM2, CNRS, UMR 7036, Institut Jean Barriol, Faculté des Sciences et Techniques, 54506 Vandoeuvre-les-Nancy, France

<sup>c</sup> Aix-Marseille Université, Service de Néphrologie, Hôpital de la Conception, Bd Baille, 13005 Marseille, France

### ARTICLE INFO

#### Article history:

Received 7 March 2014

Received in revised form

7 May 2014

Accepted 12 May 2014

Available online 24 May 2014

#### Keywords:

Nanons

Nanobacteria

CPP

Self-propagating proteins

Fetuin A

Calcification

### ABSTRACT

“Nanobacteria”, also known as nanons or calciprotein particles (CPP), are nano-sized protein mineral complexes which have been isolated from numerous biological sources. Nanons possess self-replication properties and contain only serum proteins (e.g. Fetuin-A, Albumin). Herein, we develop a simplified *in vitro* model of nanons propagation composed of only fetuin-A as a protein. Using this model, we demonstrate that fetuin from nanons possesses a different, non-native conformation. Moreover, we show that nanons induce soluble fetuin-A precipitation which could serve as a template for calcification. This phenomenon explains the observed self-propagating properties that mimic infectious behavior. We also demonstrate that renal calculi are capable of inducing a conformational change in fetuin-A, suggesting that the propagation phenomenon of nanons may occur *in vivo*.

© 2014 The Authors. Published by Elsevier Ltd. This is an open access article under the CC BY-NC-ND license (<http://creativecommons.org/licenses/by-nc-nd/3.0/>).

## 1. Introduction

Nanons or calcifying nanoparticles (CNP) are small coccoid-shaped calciparticles (0.2–0.5  $\mu\text{m}$  in diameter) that were first discovered as blood product contaminants [1]. Since then, they have been reported to be easily isolated from various sources (e.g. commercial culture medium, sera from various mammals, renal calculi, placenta, saliva, and coronary artery calcification) [2].

Nanons can be cultivated and multiplied like bacteria and have been considered as the smallest life form on earth [1]. Thus, these particles have been dubbed “nanobes” or “nanobacteria”. Nevertheless, evidences demonstrate that nanons cannot be considered as living organisms. First, nanons do not possess nucleic acid or 16sRNA [3–5], and thus their propagation is resistant to both DNase and RNase [3]. Second, nanons are more than a ten times smaller than bacteria and barely ten times bigger than ribosomes, a size incompatible with known metabolic machinery [3]. Finally, nanons can be cultivated after  $\gamma$ -irradiation of serum [1,6] and are resistant

to 90 °C heating for 1 h, treatments that would kill typical bacteria. Despite all this evidence, the controversy remains. Indeed, some authors continue to affirm that nanons are living particles [2,7,8].

To explain nanon formation, two theories have been proposed [9]. The first hypothesized a precipitation process of calcium phosphate and a calcium-binding inhibitor factor (such as fetuin-A or albumin) [9]. The second proposes a transmissible conformational change in fetuin-A, reversing its anti-precipitation properties [3]. In both hypotheses, it is proposed that fetuin-A is the key to nanon formation.

Fetuin-A is a ~360 residues glycoprotein that is present in circulating blood and is synthesized by hepatocytes. Fetuin-A is composed of 3 domains, two of which are homologous to cystatin, a protein with affinity towards hydroxyapatite salts that prevents crystal growth [10,11]. Thus, fetuin-A inhibits soft tissue calcification by forming a soluble colloidal microsphere of fetuin A–calcium phosphate complex in the blood stream [12]. Computer-modeled domain structures suggest that a dense array of acidic residues on an extended beta-sheet of the cystatin-like domain mediates efficient inhibition of calcification [13]. Although evidence suggests the involvement of fetuin-A in calcification processes, there are also many discordant findings regarding this molecular relationship [14].

Many studies in the literature report a significant role for nanons in the etiopathogenesis of various diseases, particularly related to

\* Corresponding author. URMITE, UMR CNRS 7278, IRD 198, INSERM U1095, Faculté de Médecine, 27 Bd Jean Moulin, 13385 Marseille Cedex 5, France. Tel.: +33 (0)4 91 32 43 75; fax: +33 (0)4 91 38 77 72.

E-mail address: [didier.raoult@gmail.com](mailto:didier.raoult@gmail.com) (D. Raoult).

<sup>1</sup> These two authors contributed equally to this work.

pathological calcification. Nanons serve as nidi for calcification and consequently promote it [15]. Indeed, nanons have been isolated from most kidney stones [15–17], from gallstones [18], from calcification in aortic valves or vessels [19–22], and from placenta [7,23]. These relationships were confirmed *in vivo* using animal models; injection of nanons into an animal induces calcification of tissues such as kidney [22,24] or aorta [25]. Consequently, nanons are considered to be new agents of emerging infectious diseases. In this article, we investigate the role of fetuin-A in nanon propagation using a medium containing fetuin-A as the sole source of protein.

## 2. Material and methods

### 2.1. Nanons culture

The “strain” of nanons used in this work was obtained from BioMerieux (Marcy L'étoile, Lyon, France). The nanons were propagated in 0.2  $\mu\text{m}$  sterile-filtered Dulbecco's Modified Eagle Medium (DMEM, Invitrogen, Peisley, UK) with high glucose (4.5 g/L) and depleted in sodium pyruvate. This medium was supplemented with 0.7 mM of  $\text{CaCl}_2$  (Sigma–Aldrich, Lyon, France) and with 1 mg/ml of bovine fetuin-A (Alpha-diagnostics, Texas, USA). These particles were subcultured after 2–3 weeks by diluting the culture 1:10 (v:v) in the same medium. After 5 passages, they were harvested.

### 2.2. Preparation of nanons samples for 2D SDS-PAGE and Western-blot

Flasks containing nanons were scraped; the resulting suspension was centrifuge at 12,000 rpm during 30 min and washed with Phosphate Buffer Saline (PBS). Nanons were then decalcified with EDTA 0.5 M at pH 8.9 during 4–6 h under shaking, and then dialyzed overnight against 1 L of 10 mM of PBS pH 7.5 at 4 °C using Spectra/por2 Dialysis Membrane (12–14 kDa molecular weight cut-off, Spectrum Laboratories, CA, USA). These decalcified particles containing only proteins were used for structural and biochemical analysis. The same extraction protocol was performed for renal calculi.

### 2.3. 2D SDS-PAGE and Western-blot

Extracted proteins from nanons were analyzed by 2D SDS-PAGE and Western blotting as previously described [26]. Proteins extracted from renal calculi were analyzed by Western-blot as previously described, using anti-human fetuin (1:10,000) antibodies (Santa Cruz Biotechnology, Heidelberg, Germany) [3].

### 2.4. Circular dichroism

Native bovine fetuin-A was put in contact with 10 mM of PBS and 10 mM  $\text{CaCl}_2$  (Sigma–Aldrich, Lyon, France) during 1 h. Then, native bovine fetuin-A was decalcified using the same protocol as fetuin-A extracted from nanons. Both fetuin-A (decalcified and extracted from nanons) were dialyzed overnight at 4 °C against 10 mM of PBS (pH 7.5). CD spectra were recorded at 20 °C on a Jasco 810 dichrograph equipped with a Peltier thermo-regulator, using a 1 mm thick quartz cells [27]. Spectra were measured between 190 and 260 nm with a scanning speed of 20 nm/min and a data pitch of 0.2 nm. Mean residual ellipticity ( $[\theta]$ ) were calculated as  $([\theta]) = m\Delta A/(cn)$ ,  $\Delta A$  (difference of absorption between samples and buffer),  $n$  (number of residues),  $m$  (molecular mass in Daltons), and  $c$  (protein concentration in mg/ml). Spectra were performed in triplicate at 0.1 mg/L.

The same protocol was used for fetuin-A extracted from renal calculi; excepting that native bovine fetuin-A (0.05 mg/ml) was

incubated with renal calculi for 1 week and pelleted at room temperature (RT). The supernatant was used for circular dichroism. The experimental data (in the 190–260 nm range) were analyzed using DICHROWEB [28]. The CDSSTR deconvolution method was used to estimate the content in  $\alpha$ -helical and disordered structure using the reference protein set 7. The reconstructed curves superimposed well on the experimental ones, attesting the reliability of the inferred secondary structure percentages (data not shown).

### 2.5. Precipitation assay

Native bovine fetuin-A (at 1 mg/ml) was incubated with approximately 25  $\mu\text{g}$  of nanons. The mixture was placed in PBS at RT for 1 week. The concentration of soluble protein was checked each day using a Bradford assay (Bio-Rad, Marnes La Coquette, France); the  $\text{OD}_{595\text{nm}}$  was measured using a microplate reader (Synergy HT, Biotek, USA).

### 2.6. Transmission electron microscopy tomography

Nanons were sonicated for 10 min on ice and fixed in 3% glutaraldehyde overnight at 4 °C before being placed on formvar carbon film on 400 mesh nickel grids (FCF400-Ni, EMS). Grids were treated with 1% molybdate solution in filtered water at RT. Transmission electron microscopy (TEM) tilt series were acquired with a  $\text{G}^{20}$  Cryo (FEI) for a tilt range of 100° with 2° increments. The acceleration voltage was 200 keV. The applied defocus was  $-2 \mu\text{m}$ . The magnification was 100,000.

### 2.7. Powder X-ray measurements

A solution of nanons was left to evaporate overnight at 50 °C on a zero-background X-ray holder to obtain a flat and homogeneous film on the surface. Powder X-ray measurements were performed using a Panalytical X'Pert PRO diffractometer on a reflection spinner equipped with a Cu tube ( $K\alpha_1$  ray, 0.15406 nm), a Ge(111) monochromator and an X'Celerator detector. Data collection was conducted in the scattering angle range of 5–70° with a 0.0167° step over 15 h. Crystalline phases present in the sample were identified by searching the powder diffraction file database (pdf4) using the X'Pert High Score Plus version 2.2a PANalytical software.

### 2.8. Tomographic reconstruction

Tilt series were aligned using ETomo from the IMOD software package (University of Colorado, USA) [29] by cross-correlation. The tomograms were then reconstructed using the weighted-back projection algorithm in ETomo from IMOD. The isosurfaces of the nanons were generated with 3Dmod in IMOD. The images were prepared for presentation with ImageJ (NIH).

### 2.9. Self-propagation assay

The culture of nanon-like particles (NLPs) was performed as previously described by Young et al. [9]. Briefly, the NLPs were obtained in DMEM supplemented with 10 mM each of  $\text{NaH}_2\text{PO}_4$ ,  $\text{Na}_2\text{CO}_3$ , and  $\text{CaCl}_2$  and 1 mg/ml of protein (lysozyme, fetuin-A or bovine serum albumin). After 24 h of incubation under the same condition as nanons, the NLPs were used to inoculate the same medium as described above (*i.e.* DMEM supplemented with 10 mM of  $\text{NaH}_2\text{PO}_4$ ,  $\text{Na}_2\text{CO}_3$ , and  $\text{CaCl}_2$  and 1 mg/ml of protein). The turbidity ( $\text{OD}_{600\text{nm}}$ ) was measured using a microplate reader (Synergy HT, Biotek, USA) during 14 days.

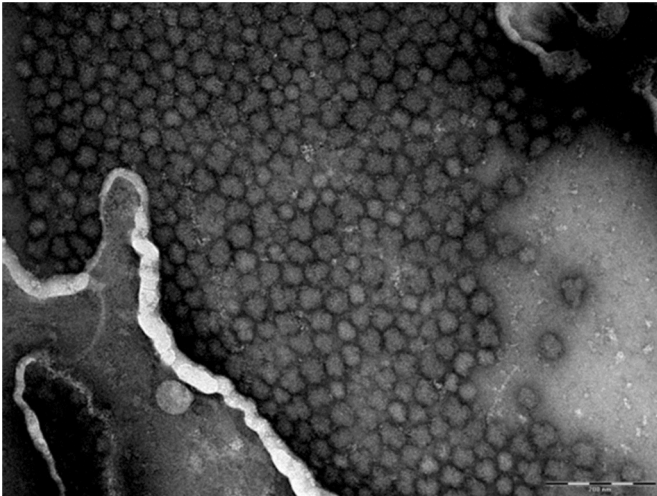


**Fig. 1.** Identification of a new invasive particle in BioMerieux culture samples. Electron micrograph of MRC-5 cells infected with nanons from BioMerieux (bar = 200 nm).

### 3. Results

#### 3.1. Particles obtained from BioMerieux are nanon-like particles

In 2008, we received cell samples from the BioMerieux laboratory that seemed to be infected with an infectious agent. These MRC-5 fibroblast cells displayed reduced growth leading to a premature death. Electron microscopic examination of the “contaminated” cells showed that they were invaded by particles resembling very small bacteria (Fig. 1). Nevertheless, 16S rDNA amplification

was negative, suggesting a non-living invasive agent (data not shown).

Because these particles closely resembled nanobacteria-like particles, we decided to characterize them. Observation of the particles by electron microscopy revealed a small size of approximately 0.2  $\mu\text{m}$  (Fig. 2A), closely resembling calcification. Tomographic reconstruction showed that the nanons had a “sponge-like” structure (Video 1). Interestingly, some regions were more electron dense (shown in yellow, Fig. 2B and Video 2). X-ray diffraction analysis showed a peak at  $32^\circ$ , characteristic of hydroxyapatite ( $\text{Ca}_{10}(\text{OH})_2(\text{PO}_4)_6$ ), while the peak width suggested that it was (nano)crystallized (Fig. 2C). The presence of hydroxyapatite can explain the high densities of some regions shown in Fig. 2B.

Supplementary data related to this article can be found online at <http://dx.doi.org/10.1016/j.micpath.2014.05.003>.

One of the major properties of nanons is their self-replication ability. We verified this property by measuring the  $\text{OD}_{600\text{nm}}$  over a 14-day period in a medium promoting nanon growth (see **Material and methods**). After 6–7 days, we observed a rise in the  $\text{OD}_{600\text{nm}}$ , suggesting “growth” (Fig. 2D). After propagation in a cell-free medium containing serum, nanons were grown in serum-free medium containing fetuin-A as the sole source of protein. After 5 passages, the protein composition of the fetuin-A-grown particles was analyzed on 2D gels and by Western blotting, revealing that these particles were solely composed of fetuin-A protein (Fig. 3A).

#### 3.2. Fetuin-A extracted from nanons possesses a different conformation

We successfully propagated nanons in a medium that contained fetuin-A as the sole source of protein. To then elucidate the

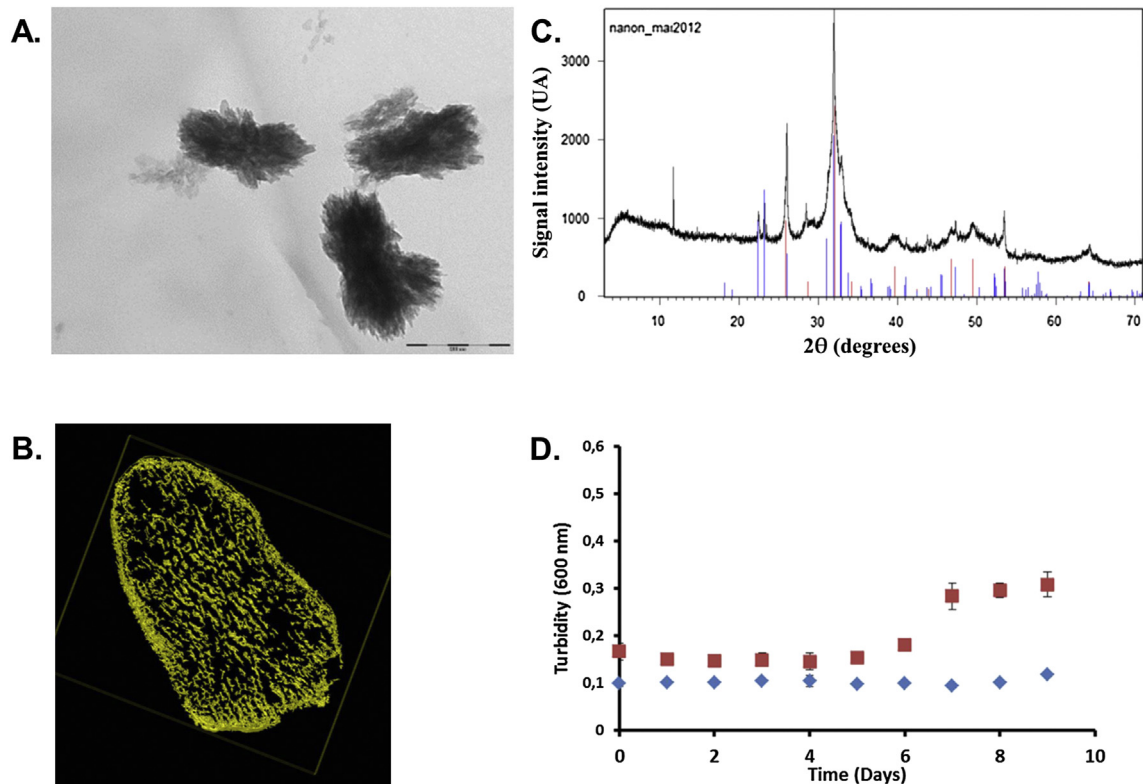


**Fig. 2.** Characterization of the isolated particle from BioMerieux. A. Electron micrographs corresponding to nanons (upper figure, bar = 200 nm). B. Tomography reconstruction. The high-density regions corresponding to hydroxyapatite are highlighted in yellow. C. Powder X-ray diffraction spectrum. Blue lines correspond to the characteristic peaks of the buffer whereas the red lines correspond to the peaks from nanons. D. Measurement of the  $\text{OD}_{600\text{nm}}$  over time. The red squares represent the  $\text{OD}_{600\text{nm}}$  of a culture of nanons whereas the blue diamonds represent the  $\text{OD}_{600\text{nm}}$  of medium alone. (For interpretation of the references to color in this figure legend, the reader is referred to the web version of this article.)

molecular mechanism of nanon formation, we extracted fetuin-A from nanons. We used circular dichroism to compare the secondary structures of native fetuin-A and the fetuin-A, we extracted from nanons. Both populations of fetuin-A clearly exhibited 2 different spectra. Indeed, compared to native fetuin-A, the nanon-derived fetuin-A spectrum showed a decrease in the mean residual ellipticity between 230 and 210 nm and a shift toward a lower wavelength of the peak with the lowest mean residual ellipticity (Fig. 3B). This shift was confirmed by an 8-nm shift at absorbance zero (in the range of 193–201 nm). Spectrum deconvolution using the DICHROWEB server [12] highlighted secondary structure differences of approximately 15–20% (Fig. 3C). This clear difference suggests an alternative conformation of nanon fetuin-A compared to native fetuin-A. This observation is not due to a bias elicited by the decalcification process, as we can clearly see that native fetuin-A and decalcified fetuin-A show similar spectra (Fig. 3B). Finally, incubation of native fetuin-A with calcified nanons led to increased aggregation of soluble native fetuin-A compared to native fetuin-A alone (Fig. 4).

### 3.3. Renal calculi change the conformation of native fetuin-A

Because early work on nanons was performed on renal calculi [13], we tested whether such calculi could stimulate a fetuin-A conformational change. First, the presence of fetuin-A in selected renal calculi was checked by Western blotting (Fig. 5A). We then incubated the remaining renal calculi with soluble native fetuin-A for 7 days before performing circular dichroism. The circular

dichroism analysis revealed a fetuin-A conformational change similar to that of the nanon-derived fetuin-A conformation (Fig. 5B).

## 4. Discussion

In 2008, the BioMerieux laboratory was contaminated by an unknown agent. Indeed, infected cells at BioMerieux displayed premature death, forcing BioMerieux to discard numerous batches of cells and causing a large economic issue. Astonishingly, BioMerieux was unable to amplify 16S rDNA from the contaminants, confusing researchers.

Using electron microscopy, we analyzed samples from BioMerieux and revealed particles closely resembling nanons. These particles were confirmed to be infectious, as they infected fibroblasts in 9 different experiments (data not shown). However, in our experience, nanon isolation is a rare event [30]; it has never happened in our broad experience of fibroblast cell culturing from human samples without anti-microbial agents, despite testing 2207 human samples including blood, cardiac valves, cerebrospinal fluid and others [31]. Clearly, nanon propagation after addition of an inoculum mimics contamination by infectious agents (*e.g.* bacteria).

### 4.1. Authentic nanons display 3 main properties

To be considered as nanons, 3 conditions must be satisfied: (1) a size of under 200 nm in diameter, which allows them to be filtrable

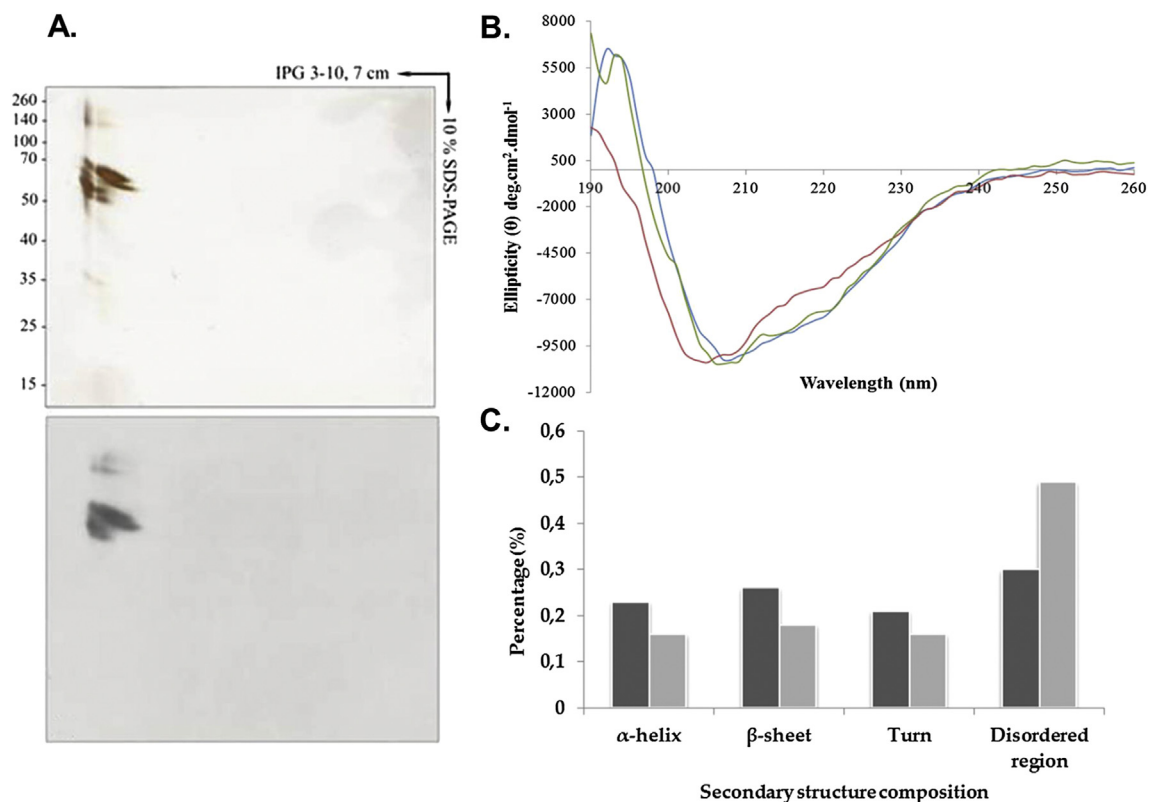


**Fig. 3.** Structural analysis of fetuin-A extracted from nanons. A. Proteins were detected by silver staining (top) or transferred to nitrocellulose and probed with 1:1000 mouse anti-fetuin-A antibodies (bottom). Sizes of molecular weight standards are indicated on the left (in kilodaltons). B. Circular dichroism of native fetuin-A (in blue), native fetuin-A extracted from nanons (in red) and decalcified native fetuin-A (in green). The X-axis represents the wavelength whereas the Y-axis represents the residual mean ellipticity. C. Secondary structure composition was evaluated using the DICHROWEB server. The Y-axis represents the percentage of secondary structure whereas the X-axis represents the different secondary structures. Native fetuin-A is represented in dark gray and fetuin-A extracted from nanons in light gray. (For interpretation of the references to color in this figure legend, the reader is referred to the web version of this article.)

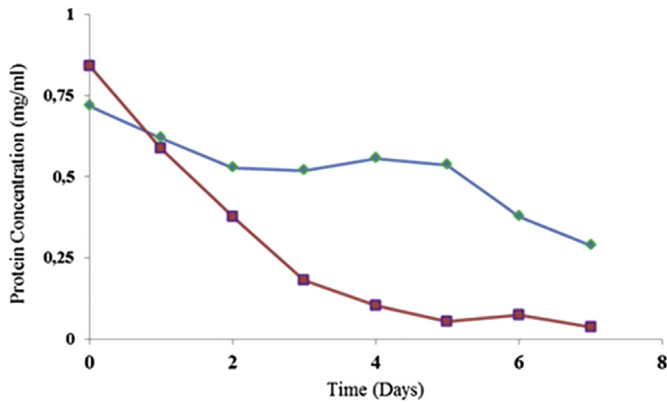


**Fig. 4.** Precipitation of soluble fetuin-A in the presence of nanons. The protein concentration (Y-axis) was estimated over the time (X-axis). Soluble native fetuin-A is represented in blue, whereas soluble native fetuin-A placed in contact with nanons is represented in red. (For interpretation of the references to color in this figure legend, the reader is referred to the web version of this article.)

at 0.2  $\mu\text{m}$ ; (2) a calcified appearance; and (3) a self-replication property without detectable nucleic acids (DNA or RNA). Young *et al.* proposed a fast protocol to cultivate nanons [9], allowing the production of small calciparticles closely resembling nanons and dubbed “nanon-like particles”. Nevertheless, we have demonstrated that these particles are not capable of self-replication (Fig. 6). The medium proposed by Young *et al.*, composed of DMEM medium supplemented with 3–10 mM  $\text{NaH}_2\text{PO}_4$  and 3–10 mM  $\text{CaCl}_2$ , is far beyond the solubility of both molecules (1 mM and 2 mM, respectively). In contrast, classical nanon culture medium contains DMEM supplemented with only 0.7 mM  $\text{CaCl}_2$  (see [Material and methods](#)). Consequently, nanon-like particles are simply calcium and phosphate salt precipitates that capture protein contained in the medium. This finding highlights the importance of checking the 3 conditions described above before concluding that a sample represents “nanons”.

Typically, two methods have been used to detect nanons [2]. First, bacterioscopic methods (*i.e.* methods classically employed for the detection of bacteria) employ electron microscopy or calcium-specific staining such as von Kossa staining. Second, bacteriological methods follow the replication of nanons. Because various mineral and mineral–protein complexes containing inorganic

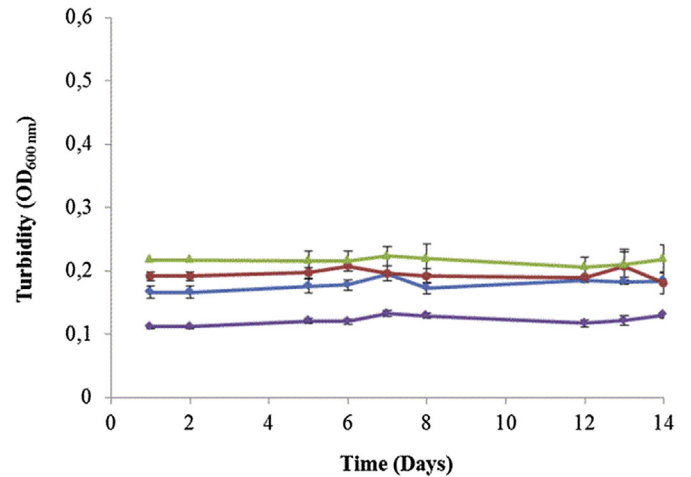


**Fig. 6.** Self-propagation assay. The turbidity of the NLP medium was plotted over time. The purple line represents the turbidity of the medium containing only DMEM with the precipitation agents (10 mM each of  $\text{NaH}_2\text{PO}_4$ ,  $\text{Na}_2\text{CO}_3$ , and  $\text{CaCl}_2$ ). Medium additionally containing 1 mg/ml of bovine fetuin-A, bovine serum albumin, and lysozyme are represented in blue, red, and green, respectively. (For interpretation of the references to color in this figure legend, the reader is referred to the web version of this article.)

calcium, phosphorus, and apatite compounds display shapes similar to the coccoid shape of nanons [3], the replication property must be verified. Numerous studies describing nanons in various tissues or environments have not checked this property, precluding a definitive conclusion about the presence of nanons.

#### 4.2. Fetuin-A from nanons changes its conformation

Here, we successfully cultivated nanons in a medium containing fetuin-A as the sole source of protein, allowing us to easily analyze the protein from nanons. Indeed, we have clearly demonstrated that fetuin-A extracted from nanons possesses a different, non-native conformation. Moreover, as the conformational change is modest (15–20%), the altered fetuin-A may retain its ability to bind hydroxyapatite.

Proteins with large numbers of acidic amino acids or phosphorylation are capable of binding hydroxyapatite and can control mineralization [32,33]. Highly glycosylated fetuin-A is also capable

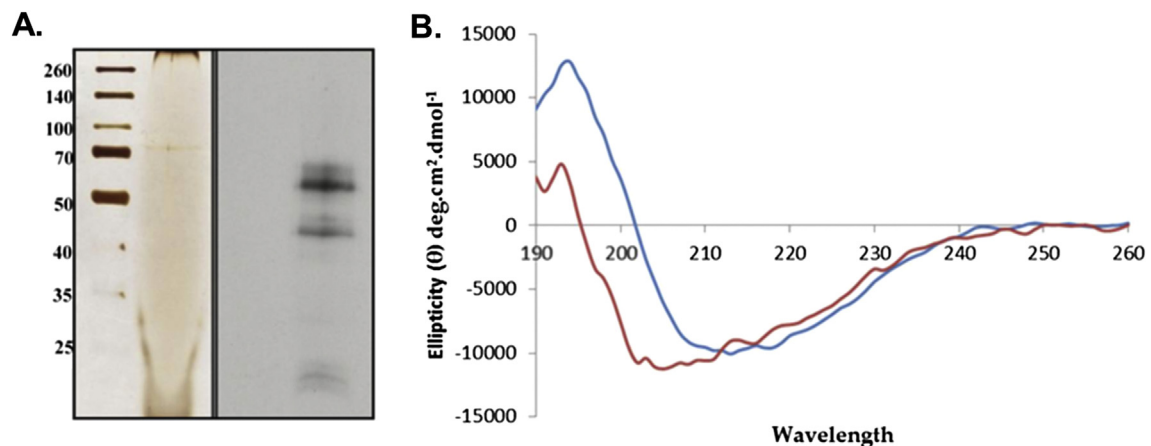


**Fig. 5.** Circular dichroism spectra of soluble fetuin-A in the presence of renal calculi containing fetuin-A. A. SDS-PAGE gel of renal calculi (left). Anti-fetuin-A (1:1000) Western blot of fetuin-A extracted from renal calculi (right). B. Circular dichroism of renal calculi incubated with fetuin-A (in red) for 1 week at room temperature. (For interpretation of the references to color in this figure legend, the reader is referred to the web version of this article.)

of binding hydroxyapatite and thus serves to prevent non-physiological mineralization by surrounding and stabilizing nascent calcium phosphate particles [34,35]. Despite its anti-precipitation properties, fetuin-A is a major component of nanons. Nanon-derived fetuin-A has a different conformation, suggesting that nanons contain pro-aggregative form of fetuin-A which self-aggregates. This aggregated fetuin-A, retaining its calcium-binding ability, could then act as a scaffold to promote calcium phosphate precipitation. *In vivo*, this precipitation process could recruit other proteins with affinity for phosphate and calcium salts (e.g. albumin) [9]. This might explain why a large number of proteins in addition to fetuin-A have been detected in nanons [2,36]. These proteins might modulate growth and shape on nanons [3].

We show that renal calculi can induce a conformational change in native fetuin-A, suggesting that nanon propagation also occurs *in vivo*. Both low and physiological fetuin-A levels in blood have been associated with formation of blood vessels calcification [37,38]. Nanons are good candidates for explaining this discrepancy, if the nanon fetuin-A conformation makes it unable to inhibit calcification.

Our results show that the fetuin-A contained in nanons possesses a different conformation than native fetuin-A. Moreover, in the presence of nanons, fetuin-A precipitates and may serve as a template for calcification, forming new nanons. Because inoculation with nanons is necessary to induce their propagation, they mimic infectious behavior. We also show that renal calculi can induce a conformational change in native fetuin-A, suggesting that nanon propagation may also occur *in vivo*. Furthermore, this phenomenon may be generalized and may explain some calcification of unknown origin described in the literature; thus, nanons should be viewed as a new infectious agent.

## Acknowledgments

The authors have declared that no competing interests exist.

## References

- [1] Kajander EO, Kuronen I, Akerman KK, Pelttari A, Ciftcioglu N. Nanobacteria from blood: the smallest culturable autonomously replicating agent on earth; 1997. pp. 420–8.
- [2] Kutikhin AG, Brusina EB, Yuzhalin AE. The role of calcifying nanoparticles in biology and medicine. *Int J Nanomed* 2012;7:339–50.
- [3] Raoult D, Drancourt M, Azza S, Nappes C, Guieu R, Rolain JM, et al. Nanobacteria are mineralo fetuin complexes. *PLoS Pathog* 2008;4:e41.
- [4] Barba I, Villacorta E, Bratos-Perez MA, Antolin M, Varela E, Sanchez PL, et al. Aortic valve-derived calcifying nanoparticles: no evidence of life. *Rev Esp Cardiol* 2012;65:813–8.
- [5] Cisar JO, Xu DQ, Thompson J, Swaim W, Hu L, Kopecko DJ. An alternative interpretation of nanobacteria-induced biomineralization. *Proc Natl Acad Sci U S A* 2000;97:11511–5.
- [6] Martel J, Wu CY, Young JD. Critical evaluation of gamma-irradiated serum used as feeder in the culture and demonstration of putative nanobacteria and calcifying nanoparticles. *PLoS One* 2010;5:0010343.
- [7] Lu H, Guo YN, Liu SN, Zhang DC. Nanobacteria may be linked to calcification in placenta. *Ultrastruct Pathol* 2012;36:160–5.
- [8] Lu H, Guo YN, Liu SN, Zhu H, Zhang DC. Isolation, cultivation and identification of nanobacteria from placental calcification. *J Matern Fetal Neonatal Med* 2012;25:2182–5.
- [9] Young JD, Martel J, Young L, Wu CY, Young A, Young D. Putative nanobacteria represent physiological remnants and culture by-products of normal calcium homeostasis. *PLoS One* 2009;4:e4417.
- [10] Vitorino R, Lobo MJ, Duarte J, Ferrer-Correia AJ, Tomer KB, Dubin JR, et al. *In vitro* hydroxyapatite adsorbed salivary proteins. *Biochem Biophys Res Commun* 2004;320:342–6.
- [11] Armstrong WG. Characterisation studies on the specific human salivary proteins adsorbed *in vitro* by hydroxyapatite. *Caries Res* 1971;5:215–27.
- [12] Mosa OF, Mohamad IH, Salama MM. Relationship between fetuin-A and systemic lupus erythematosus as a predictor marker for atherosclerosis. *Am Med J*; 2012;249–54.
- [13] Heiss A, DuChesne A, Denecke B, Grotzinger J, Yamamoto K, Renne T, et al. Structural basis of calcification inhibition by alpha 2-HS glycoprotein/fetuin-A. Formation of colloidal calciprotein particles. *J Biol Chem* 2003;278:13333–41.
- [14] Mori K, Emoto M, Inaba M. Fetuin-A and the cardiovascular system. *Adv Clin Chem* 2012;56:175–95.
- [15] Ciftcioglu N, Bjorklund M, Kuorikoski K, Bergstrom K, Kajander EO. Nanobacteria: an infectious cause for kidney stone formation. *Kidney Int* 1999;56:1893–8.
- [16] Kajander EO, Ciftcioglu N. Nanobacteria: an alternative mechanism for pathogenic intra- and extracellular calcification and stone formation. *Proc Natl Acad Sci U S A* 1998;95:8274–9.
- [17] Khullar M, Sharma SK, Singh SK, Bajwa P, Sheikh FA, Relan V, et al. Morphological and immunological characteristics of nanobacteria from human renal stones of a north Indian population. *Urol Res* 2004;32:190–5.
- [18] Wang L, Shen W, Wen J, An X, Cao L, Wang B. An animal model of black pigment gallstones caused by nanobacteria. *Dig Dis Sci* 2006;51:1126–32.
- [19] Miller VM, Rodgers G, Charlesworth JA, Kirkland B, Severson SR, Rasmussen TE, et al. Evidence of nanobacterial-like structures in calcified human arteries and cardiac valves. *Am J Physiol Heart Circ Physiol* 2004;287:13.
- [20] Puskas LG, Tiszlavicz L, Razga Z, Torday LL, Krenacs T, Papp JG. Detection of nanobacteria-like particles in human atherosclerotic plaques. *Acta Biol Hung* 2005;56:233–45.
- [21] Bratos-Perez MA, Sanchez PL, Garcia de Cruz S, Villacorta E, Palacios IF, Fernandez-Fernandez JM, et al. Association between self-replicating calcifying nanoparticles and aortic stenosis: a possible link to valve calcification. *Eur Heart J* 2008;29:371–6.
- [22] Hu WG, Wang XF, Xu T, Li JX, Chen L, Yu CF, et al. Establishment nephrolithiasis rat model induced by nanobacteria and analysis of stone formation. *Beijing Da Xue Xue Bao* 2010;42:433–5.
- [23] Agababov RM, Abashina TN, Suzina NE, Vainshtein MB, Schwartzburd PM. Link between the early calcium deposition in placenta and nanobacterial-like infection. *J Biosci* 2007;32:1163–8.
- [24] Shiekh FA, Khullar M, Singh SK. Lithogenesis: induction of renal calcifications by nanobacteria. *Urol Res* 2006;34:53–7.
- [25] Schwartz MA, Lieske JC, Kumar V, Farell-Baril G, Miller VM. Human-derived nanoparticles and vascular response to injury in rabbit carotid arteries: proof of principle. *Int J Nanomed* 2008;3:243–8.
- [26] Azza S, Cambillau C, Raoult D, Suzan-Monti M. Revised mimivirus major capsid protein sequence reveals intron-containing gene structure and extra domain. *BMC Mol Biol* 2009;10:39.
- [27] Habchi J, Blangy S, Mamelli L, Jensen MR, Blackledge M, Darbon H, et al. Characterization of the interactions between the nucleoprotein and the phosphoprotein of Henipavirus. *J Biol Chem* 2011;286:13583–602.
- [28] Lobley A, Whitmore L, Wallace BA. DICHROWEB: an interactive website for the analysis of protein secondary structure from circular dichroism spectra. *Bioinformatics* 2002;18:211–2.
- [29] Kremer JR, Mastrorade DN, McIntosh JR. Computer visualization of three-dimensional image data using IMOD. *J Struct Biol* 1996;116:71–6.
- [30] Drancourt M, Jacomo V, Lepidi H, Lechevallier E, Grisoni V, Coulangue C, et al. Attempted isolation of *Nanobacterium* sp. microorganisms from upper urinary tract stones. *J Clin Microbiol* 2003;41:368–72.
- [31] Gouriet F, Fenollar F, Patrice JY, Drancourt M, Raoult D. Use of shell-vial cell culture assay for isolation of bacteria from clinical specimens: 13 years of experience. *J Clin Microbiol* 2005;43:4993–5002.
- [32] Weiner S, Addadi L. Acidic macromolecules of mineralized tissues: the controllers of crystal formation. *Trends Biochem Sci* 1991;16:252–6.
- [33] Hunter GK, Hauschka PV, Poole AR, Rosenberg LC, Goldberg HA. Nucleation and inhibition of hydroxyapatite formation by mineralized tissue proteins. *Biochem J* 1996;317(Pt 1):59–64.
- [34] Bryllka L, Jahnen-Dechent W. The role of fetuin-A in physiological and pathological mineralization. *Calcif Tissue Int* 2013;93:355–64.
- [35] Rochette CN, Rosenfeldt S, Heiss A, Narayanan T, Ballauff M, Jahnen-Dechent W. A shielding topology stabilizes the early stage protein-mineral complexes of fetuin-A and calcium phosphate: a time-resolved small-angle X-ray study. *ChemBiochem* 2009;10:735–40.
- [36] Shiekh FA, Charlesworth JE, Kim SH, Hunter LW, Jayachandran M, Miller VM, et al. Proteomic evaluation of biological nanoparticles isolated from human kidney stones and calcified arteries. *Acta Biomater* 2010;6:4065–72.
- [37] Ketteler M, Bongartz P, Westenfeld R, Wildberger JE, Mahnken AH, Bohm R, et al. Association of low fetuin-A (AHSG) concentrations in serum with cardiovascular mortality in patients on dialysis: a cross-sectional study. *Lancet* 2003;361:827–33.
- [38] Price PA, Williamson MK, Nguyen TM, Than TN. Serum levels of the fetuin-mineral complex correlate with artery calcification in the rat. *J Biol Chem* 2004;279:1594–600.